

Chapter 2

Schottky Rectifiers

A Schottky rectifier is formed by making an electrically non-linear contact between a metal and the semiconductor drift region. The Schottky rectifier is an attractive unipolar device for power electronics applications due to its relatively low on-state voltage drop and its fast switching behavior. It has been widely used in power supply circuits with low operating voltages due to the availability of excellent devices based upon silicon technology. In the case of silicon, the maximum breakdown voltage of Schottky rectifiers has been limited by the increase in the resistance of the drift region. Commercially available devices are generally rated at breakdown voltages of less than 100 volts.

Many applications described in chapter 1 require fast switching rectifiers with low on-state voltage drop that can also support over 500 volts. The much lower resistance of the drift region for silicon carbide enables development of such Schottky rectifiers with very high breakdown voltages¹. These devices not only offer fast switching speed but also eliminate the large reverse recovery current observed in high voltage silicon P-i-N rectifiers. This reduces switching losses not only in the rectifier but also in the IGBTs used within the power circuits².

In this chapter, the basic structure of the power Schottky rectifier is first introduced to define its constituent elements. The current transport mechanisms that are pertinent to power devices are elucidated for both the forward and reverse mode of operation. In the first quadrant of operation, the thermionic emission process is dominant for power Schottky rectifiers. In the third quadrant of operation, the influence of Schottky barrier lowering has a strong impact on the leakage current for silicon devices. In the case of silicon carbide devices, the influence of tunneling current must also be taken into account when performing the analysis of the reverse leakage current.

The information in this chapter is intended to provide the context and perspective for the discussion of advanced device concepts in subsequent chapters. A more detailed discussion of the fundamental concepts relevant to power Schottky rectifiers is provided in a recently published textbook³. This includes optimization of the Schottky barrier height depending upon the duty cycle and the maximum junction temperature.

2.1 Power Schottky Rectifier Structure

The basic one-dimensional structure of the metal-semiconductor or Schottky rectifier structure is shown in Fig. 2.1 together with electric field profile under reverse bias operation. The applied voltage is supported by the drift region with a triangular electric field distribution if the drift region doping is uniform. The maximum electric field occurs at the metal contact. The device undergoes breakdown when this field becomes equal to the critical electric field for the semiconductor.

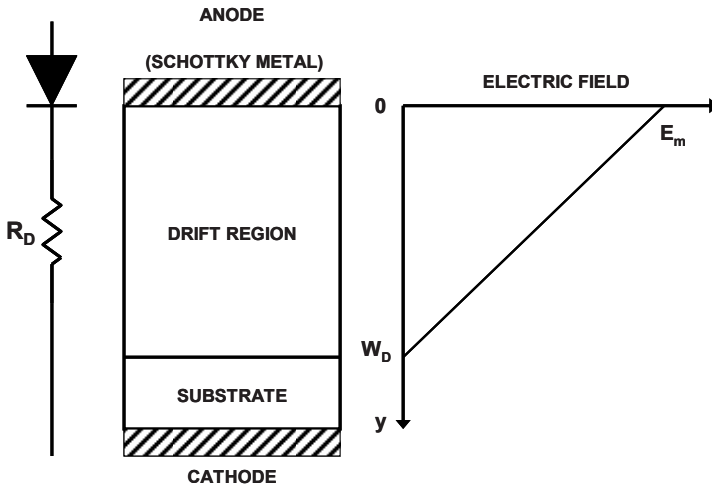


Fig. 2.1 Electric Field Distribution in a Schottky Rectifier.

When a negative bias is applied to the cathode, current flow occurs in the Schottky rectifier by the transport of electrons over the metal-semiconductor contact and through the drift region as well as the substrate. The on-state voltage drop is determined by the voltage drop across the metal-semiconductor interface and the ohmic voltage drop in the resistance of the drift region, the substrate and its ohmic contact.

At typical on-state operating current density levels, the current transport is dominated by majority carriers. Consequently, there is insignificant minority carrier stored charge within the drift region in the power Schottky rectifier. This enables switching the Schottky rectifier from the on-state to the reverse blocking

off-state in a rapid manner by establishing a depletion region within the drift region. The fast switching capability of the Schottky rectifier enables operation at high frequencies with low power losses making this device popular for high frequency switch mode power supply applications. With the advent of commercially available high voltage Schottky rectifiers based upon silicon carbide, they are expected to be utilized in motor control applications as well.

A useful relationship for obtaining the Schottky barrier height is:

$$\Phi_{BN} = \Phi_M - \chi_S \quad [2.1]$$

where ϕ_M is the metal work function and χ_S is the electron affinity of the semiconductor. The potential difference between the Fermi level in the semiconductor (E_{FS}) and the Fermi level in the metal (E_{FM}) is called the *contact potential* (V_C) which is given by:

$$qV_C = (E_{FS} - E_{FM}) = \Phi_M - \Phi_S = \Phi_M - (\chi_S + E_C - E_{FS}) \quad [2.2]$$

where ϕ_S is the semiconductor work function and E_C is the conduction band edge. The built-in potential (V_{bi}) at the Schottky contact (equal to the contact potential) creates a depletion region within the semiconductor at zero bias given by:

$$W_0 = \sqrt{\frac{2\epsilon_S V_{bi}}{qN_D}} \quad [2.3]$$

2.2 Forward Conduction

Current flow across the metal-semiconductor junction can be produced by the application of a negative bias to the N-type semiconductor region. Current flow across the interface then occurs mainly due to majority carriers – electrons for the case of an N-type semiconductor. The current flow via the thermionic emission process is the dominant current transport mechanism in silicon and silicon carbide Schottky power rectifiers. In the case of high mobility semiconductors, such as silicon, gallium arsenide and silicon carbide, the thermionic emission theory can be used to describe the current flow across the Schottky barrier interface⁴:

$$J = AT^2 e^{-(q\Phi_{BN} / kT)} \left[e^{(qV / kT)} - 1 \right] \quad [2.4]$$

where A is the effective Richardson's constant, T is the absolute temperature, k is Boltzmann's constant, and V is the applied bias. An effective Richardson's constant of 110, 140, and 146 A/cm²-°K² can be used for n-type silicon⁶, gallium arsenide⁶, and 4H silicon carbide³, respectively. This expression, based upon the superimposition of the current flux from the metal and the semiconductor⁵ which balance out at zero bias, holds true for both positive and negative voltages applied to the metal contact.

When a forward bias is applied (positive values for V in Eq. [2.4]), the first term in the square brackets of the equation becomes dominant allowing calculation of the forward current density:

$$J_F = AT^2 e^{-(q\Phi_{BN}/kT)} e^{(qV_{FS}/kT)} \quad [2.5]$$

where V_{FS} is the forward voltage drop across the Schottky contact. In the case of power Schottky rectifiers, a thick lightly doped drift region must be placed below the Schottky contact as illustrated in Fig. 2.1 to allow supporting the reverse blocking voltage. A resistive voltage drop (V_R) occurs across this drift region which increases the on-state voltage drop of the power Schottky rectifier beyond V_{FS} . In case of current transport by the thermionic emission process, there is no modulation of the resistance of the drift region because minority carrier injection is neglected. Due to the small thickness (typically less than 50 microns) of the drift region for power Schottky diodes, it is grown on top of a heavily doped N^+ substrate as a handle during processing and packaging of the devices. The resistance contributed by the substrate (R_{SUB}) must be included in the analysis because it can be comparable to that of the drift region especially for silicon carbide devices. In addition, the resistance of the ohmic contact (R_{CONT}) to the cathode may make a substantial contribution to the on-state voltage drop.

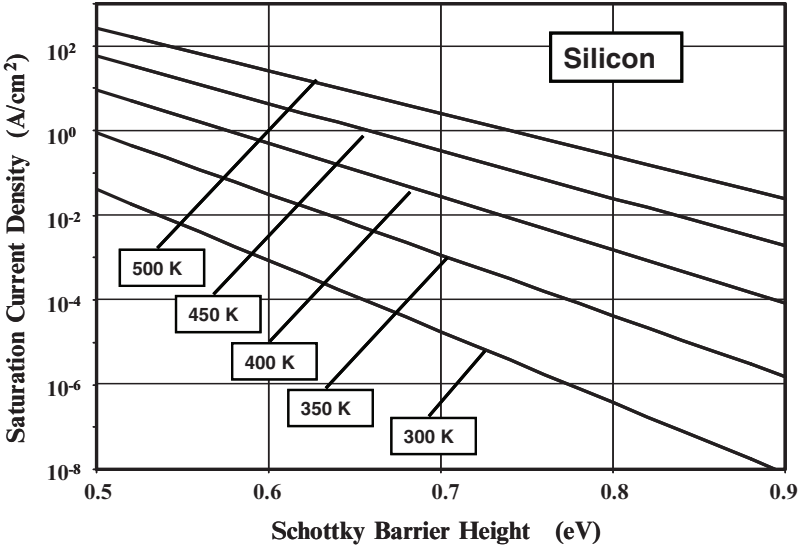


Fig. 2.2 Saturation Current Density for Silicon Schottky Barrier Rectifiers.

The on-state voltage drop (V_F) for the power Schottky rectifier, after including the resistive voltage drop, is given by:

$$V_F = V_{FS} + V_R = \frac{kT}{q} \ln \left(\frac{J_F}{J_S} \right) + R_{S,SP} J_F \quad [2.6]$$

where J_F is the forward (on-state) current density, J_S is the saturation current density, and $R_{S,SP}$ is the total series specific resistance. In this expression, the saturation current is given by:

$$J_S = AT^2 e^{-(q\Phi_{BN}/kT)} \quad [2.7]$$

and the total series specific resistance is given by:

$$R_{S,SP} = R_{D,SP} + R_{SUB} + R_{CONT} \quad [2.8]$$

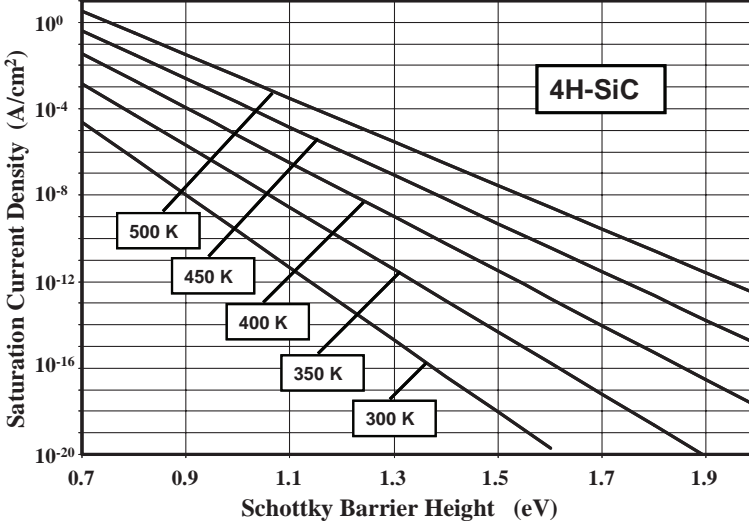


Fig. 2.3 Saturation Current Density for 4H-SiC Schottky Barrier Rectifiers.

The saturation current is a strong function of the Schottky barrier height and the temperature as shown in Fig. 2.2 for silicon devices. The barrier heights chosen for this plot are in the range for typical metal contacts with silicon. The saturation current density increases with increasing temperature and reduction of the barrier height. This has an influence not only on the on-state voltage drop but an even greater impact on the reverse leakage current as discussed in the next section. A corresponding plot is provided in Fig. 2.3 for 4H-SiC devices. A larger range of Schottky barrier heights has been selected for this graph because this is typical for the wide band gap semiconductor.

As discussed in chapter 1, the specific on-resistance of the drift region is given by:

$$R_{on-ideal} = \frac{4BV^2}{\epsilon_s \mu_n E_C^3} \quad [2.9]$$

The specific on-resistance of the drift region for 4H-SiC is approximately 2000 times smaller than for silicon devices for the same breakdown voltage. Their values are given by:

$$R_{D,SP} = R_{on-ideal}(Si) = 5.93 \times 10^{-9} BV^{2.5} \quad [2.10]$$

and

$$R_{D,SP} = R_{on-ideal}(4H-SiC) = 2.97 \times 10^{-12} BV^{2.5} \quad [2.11]$$

In addition, it is important to include the resistance associated with the thick, highly doped N^+ substrate because this is comparable to that for the drift region in some instances. The specific resistance of the N^+ substrate can be determined by taking the product of its resistivity and thickness. For silicon, N^+ substrates with resistivity of 1 m Ω -cm are available. If the thickness of the substrate is 200 microns, the specific resistance contributed by the N^+ substrate is $2 \times 10^{-5} \Omega\text{-cm}^2$. For silicon carbide, the available resistivity of the N^+ substrates is substantially larger. For the available substrates with a typical resistivity of 0.02 $\Omega\text{-cm}$ and thickness of 200 microns, the substrate contribution is $4 \times 10^{-4} \Omega\text{-cm}^2$. The specific resistance of the ohmic contact to the N^+ substrate can be reduced to less than $1 \times 10^{-6} \Omega\text{-cm}^2$ with adequate attention to increasing the doping concentration at the contact and by using ohmic contact metals with low barrier heights.

The calculated forward conduction characteristics for silicon Schottky rectifiers are shown in Fig. 2.4 for various breakdown voltages. For this figure, a Schottky barrier height of 0.7 eV was chosen because this is a typical value used in actual power devices. It can be seen that the series resistance of the drift region

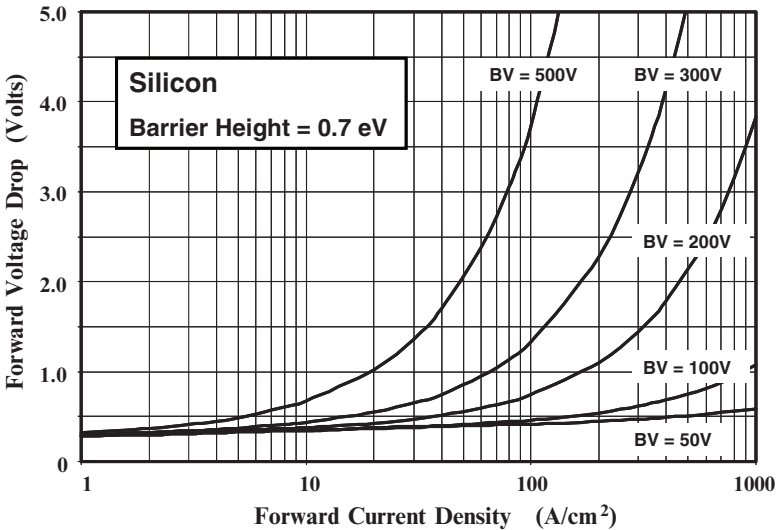


Fig. 2.4 Forward Characteristics of Silicon Schottky Rectifiers.

does not adversely impact the on-state voltage drop for the device with a breakdown voltage of 50 volts at a nominal on-state current density of 100 A/cm^2 . However, this resistance becomes significant when the breakdown voltage exceeds 100 volts, limiting the application of silicon Schottky rectifiers to systems, such as switch-mode power supply circuits, operating at voltages below 100 V.

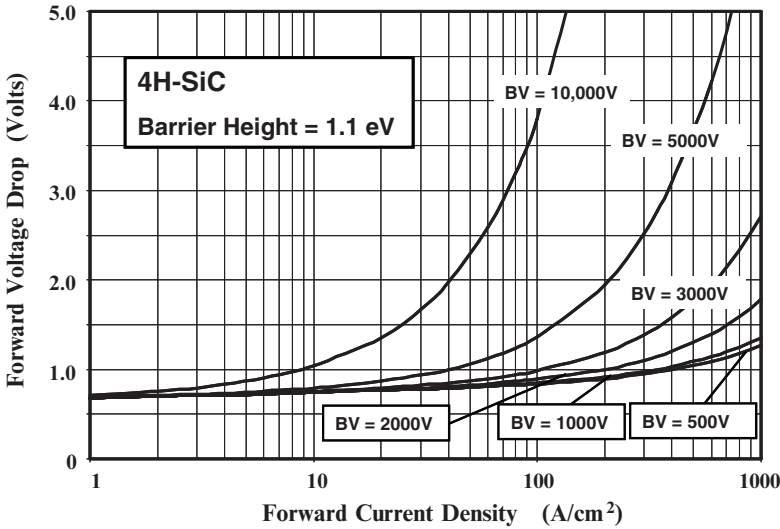


Fig. 2.5 Forward Characteristics of 4H-SiC Schottky Rectifiers.

The significantly smaller resistance of the drift region enables scaling of the breakdown voltage of silicon carbide Schottky rectifiers to much larger voltages typical of medium and high power electronic systems, such as those used for motor control. The forward characteristics of high voltage 4H-SiC Schottky rectifiers are shown in Fig. 2.5 for the case of a Schottky barrier height of 1.1 eV. The N^+ substrate resistance used for these calculations was $4 \times 10^{-4} \Omega\text{-cm}^2$. It can be seen that the drift region resistance does not produce a significant increase in on-state voltage drop until the breakdown voltage exceeds 3000 volts. From these results, it can be concluded that silicon carbide Schottky rectifiers are excellent companion diodes for medium and high power electronic systems that utilize Insulated Gate Bipolar Transistors (IGBTs). Their fast switching speed and absence of reverse recovery current can reduce power losses and improve the efficiency in motor control applications².

The choice of the Schottky barrier height has a strong impact on the on-state voltage drop. For typical power Schottky rectifiers, the on-state voltage drop increases in proportion to the magnitude of the Schottky barrier height. It is therefore attractive to use a low Schottky barrier height for power rectifiers in order to reduce the on-state voltage drop. For silicon devices with low blocking voltages, the forward voltage drop for the Schottky diode decreases with increasing

temperature due to a reduction in the voltage across the Schottky contact. For 4H-SiC Schottky rectifiers with high blocking voltages, the on-state voltage drop increases with increasing temperature due to an increase in the resistive voltage drop across the drift region. A more detailed discussion of the impact of the Schottky barrier height on the on-state voltage drop can be found in the textbook³. The design of a power Schottky rectifier for any application requires selection of the Schottky barrier height to minimize the on-state power losses while avoiding excessive leakage current in the reverse blocking mode. The reverse blocking characteristics of Schottky rectifiers are discussed in the next section.

2.3 Reverse Blocking

When a reverse bias is applied to the Schottky rectifier, the voltage is supported across the drift region with the maximum electric field located at the metal-semiconductor contact as shown in Fig. 2.1. Since no voltage can be supported within the metal, the reverse blocking capability of the Schottky rectifier is governed by the physics for the abrupt P-N junction³. If a parallel-plane breakdown voltage is assumed, the drift region doping and width for a silicon device are given by:

$$N_D = 2 \times 10^{18} (BV_{PP})^{-4/3} \quad [2.12]$$

and

$$W_D = 2.58 \times 10^{-6} (BV_{PP})^{7/6} \quad [2.13]$$

In the case of actual power Schottky rectifiers, the breakdown voltage is constrained by breakdown at the edges. Edge terminations have been developed to raise the breakdown voltage of Schottky rectifiers close to the parallel-plane value^{1,3}.

Due to the relatively small barrier height utilized in silicon Schottky rectifiers, the thermionic emission component is dominant. The leakage current for the Schottky rectifier can be obtained by using Eq. [2.4] and substituting a negative bias of magnitude V_R . The leakage current is then determined by the saturation current:

$$J_L = -AT^2 e^{-(q\Phi_{BN}/kT)} = -J_S \quad [2.14]$$

which is a strong function of the Schottky barrier height and the temperature. In order to reduce the leakage current and minimize power dissipation in the blocking state, a large Schottky barrier height is required. Further, a very rapid increase in leakage current occurs with increasing temperature, as shown in Fig. 2.6. If the power dissipation due to the leakage current becomes dominant, the resulting increase in the device temperature produces a positive feedback mechanism which can lead to unstable operation of the Schottky rectifier due to thermal runaway.

This destructive failure mechanism for power Schottky rectifiers must be avoided by sufficiently increasing the Schottky barrier height even though this increases the on-state voltage drop. A larger Schottky barrier height is warranted for power Schottky rectifiers that must operate at higher ambient temperatures. The leakage current in power Schottky rectifiers is actually much greater than the saturation current due to the Schottky barrier lowering and tunneling phenomena.

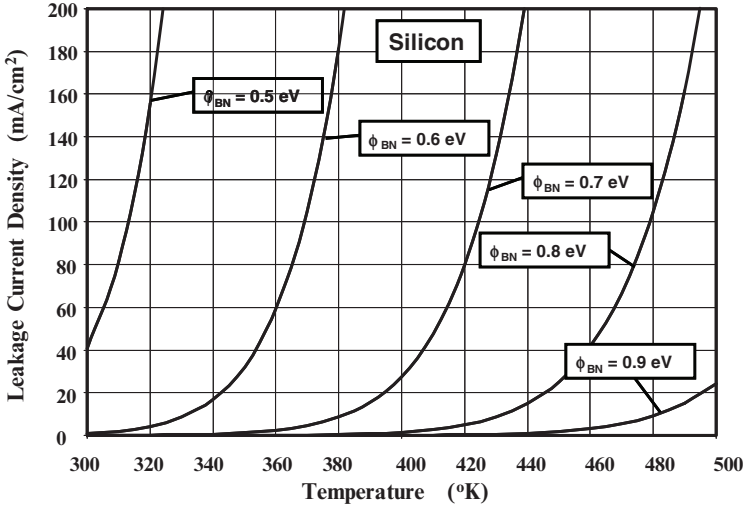


Fig. 2.6 Temperature Dependence of the Leakage Current for Silicon Schottky Rectifiers.

2.3.1 Schottky Barrier Lowering

Based upon the above analysis, the leakage current of the Schottky rectifier should be independent of the magnitude of the applied reverse bias voltage. However, actual power Schottky rectifiers exhibit a significant increase in the leakage current with increasing reverse bias voltage. This increase in the leakage current is far greater than the space charge generation current within the expanding depletion region with increasing reverse bias voltage.

Under reverse blocking operation, it has been found that there is a reduction of the Schottky barrier height due the image force lowering phenomenon⁶. The barrier lowering is found to be determined by the maximum electric field (E_M) at the metal-semiconductor interface³:

$$\Delta\phi_{BN} = \sqrt{\frac{qE_M}{4\pi\epsilon_S}} \quad [2.15]$$

For a one-dimensional structure, the maximum electric field is related to the applied reverse bias voltage (V_R) by:

$$E_M = \sqrt{\frac{2qN_D}{\epsilon_S} (V_R + V_{bi})} \quad [2.16]$$

As an example, the reductions of the barrier height for silicon and 4H-SiC Schottky rectifiers are shown in Fig. 2.7 for the case of a drift region doping concentration of $1 \times 10^{16} \text{ cm}^{-3}$. The reduction of the Schottky barrier height is 0.065 eV at the maximum reverse bias voltage for the silicon structure. Since the low specific on-resistance of the drift region in silicon carbide devices is associated with the much larger electric field in the material before the on-set of impact ionization, the Schottky barrier lowering in silicon carbide rectifiers can be expected to be significantly larger than in silicon devices. For the case of a drift region doping level of $1 \times 10^{16} \text{ cm}^{-3}$, the barrier lowering is found to be three times larger in silicon carbide at the corresponding breakdown voltage as shown in Fig. 2.7. This can lead to a much larger increase in the leakage current with increasing reverse bias voltage for silicon carbide devices. In preparing Fig. 2.7, the reverse voltage was normalized to the breakdown voltage because of the different breakdown voltages for the silicon (50 volts) and silicon carbide devices (3000 volts).

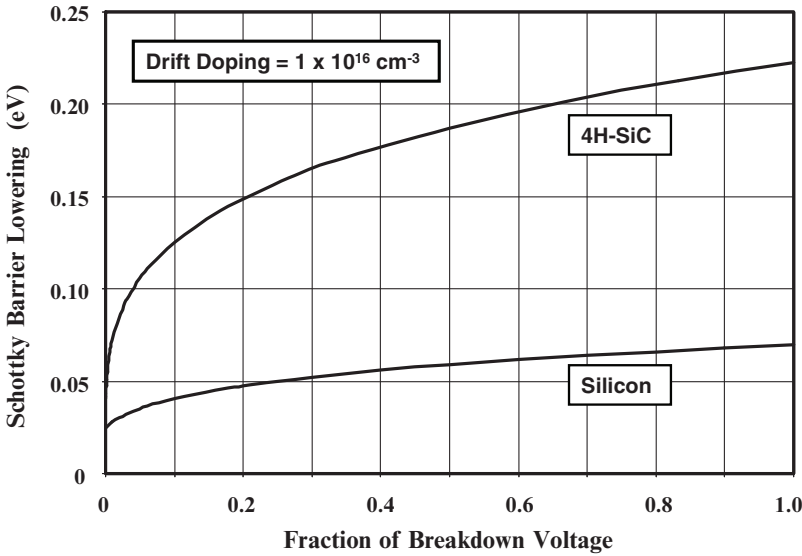


Fig. 2.7 Schottky Barrier Lowering for Silicon and 4H-SiC Schottky Rectifiers.

The leakage current for the Schottky rectifier including the effect of Schottky barrier lowering is given by:

$$J_L = -AT^2 e^{-q(\phi_{BN} - \Delta\phi_{BN})/kT} \quad [2.17]$$

The leakage currents calculated with and without the Schottky barrier lowering effect are compared for the case of a silicon device with a breakdown voltage of 50 volts in Fig. 2.8. In making these plots, the leakage current due to space-charge-generation was neglected because it is much smaller than the leakage current across the metal-semiconductor contact. It can be seen that the leakage current is enhanced by a factor of five times due to the barrier lowering phenomenon as the reverse voltage increase and approaches the breakdown voltage. The actual reverse leakage current for silicon Schottky rectifiers has been found to increase by an even greater degree than predicted by the Schottky barrier lowering phenomenon.

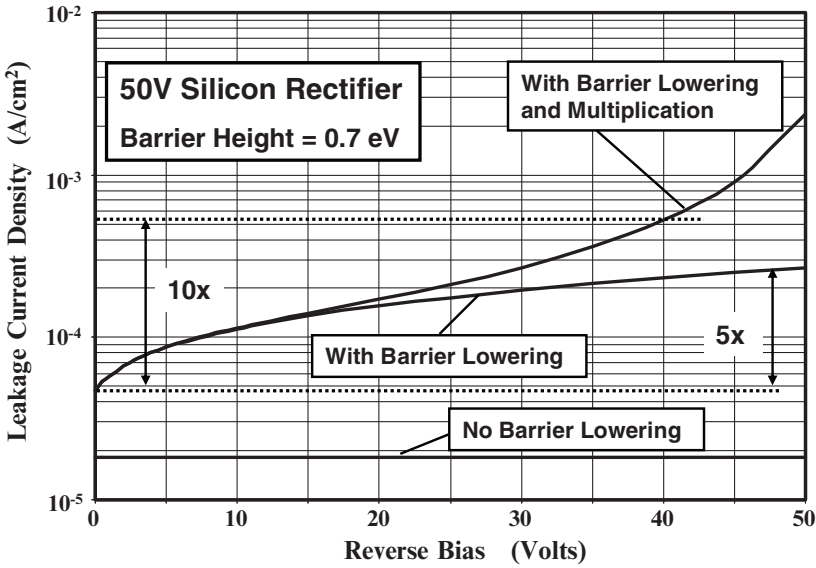


Fig. 2.8 Leakage Current Density for a 50V Silicon Schottky Rectifier.

2.3.2 Pre-Breakdown Avalanche Multiplication

The large increase in leakage current in actual silicon power Schottky rectifiers can be accounted for by including the effect of pre-breakdown avalanche multiplication of the large number of free carriers being transported through the Schottky rectifier structure at the high electric fields associated with reverse bias voltages close to the breakdown voltage⁷. The total number of electrons that reach the edge of the depletion region are larger than those crossing the metal-semiconductor contact by a factor M_n . The multiplication coefficient (M_n) is determined from the maximum electric field (E_M) at the metal-semiconductor contact:

$$M_n = \left\{ 1 - 1.52 \left[1 - \exp \left(-7.22 \times 10^{-25} E_m^{4.93} W_D \right) \right] \right\}^{-1} \quad [2.18]$$

where W_D is the depletion layer width. The leakage current density for a silicon Schottky rectifier with drift region doping concentration of $1 \times 10^{16} \text{ cm}^{-3}$ is shown in Fig. 2.8 after including the influence of the pre-breakdown multiplication coefficient. The effect of including the multiplication coefficient is apparent at high voltages when the electric field approaches the critical electric field for breakdown. The leakage currents obtained, after including the effects of Schottky barrier lowering and pre-breakdown multiplication, are consistent with the characteristics of commercially available silicon devices, which exhibit an order of magnitude increase in leakage current from low reverse bias voltages to the rated voltage (about 80 percent of the breakdown voltage).

2.3.3 Silicon Carbide Schottky Rectifiers

The enhanced Schottky barrier lowering in silicon carbide devices leads to a more rapid increase in leakage current with increasing reverse bias as shown in Fig. 2.9. The leakage current is predicted by this model to increase by about three orders of magnitude when the reverse voltage approaches the breakdown voltage. However, the observed increase in leakage current with applied reverse bias voltage for high voltage silicon carbide Schottky rectifiers is much greater than can be accounted for with the Schottky barrier lowering model^{8,9,10} despite the much larger barrier lowering effect. The experimentally observed increase in leakage current is about 6 orders of magnitude with increase in reverse bias voltage.

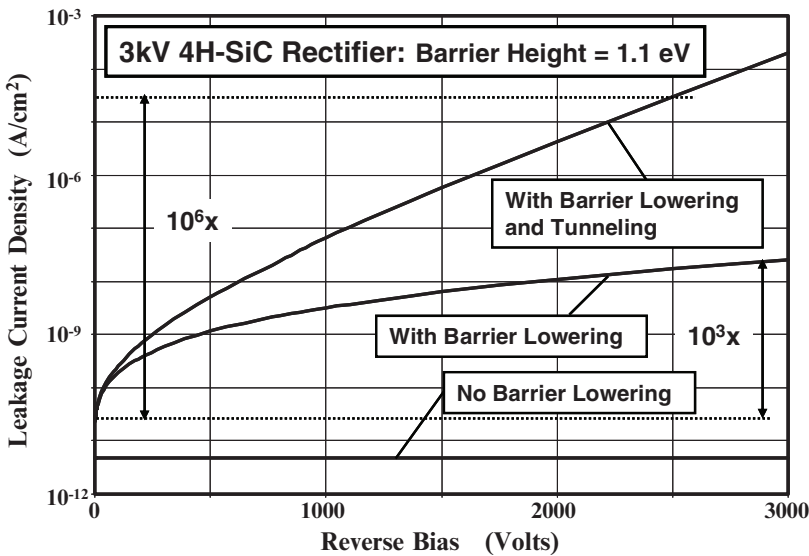


Fig. 2.9 Leakage Current Density for a 3kV 4H-SiC Schottky Rectifier.

In order to explain the more rapid increase in leakage current observed in silicon carbide Schottky rectifiers, it is necessary to include the field emission (or tunneling) component of the leakage current¹¹. The thermionic field emission model for the tunneling current leads to a barrier lowering effect proportional to the square of the electric field at the metal-semiconductor interface. When combined with the thermionic emission model, the leakage current density can be written as:

$$J_s = AT^2 \exp\left(-\frac{q\phi_{BN}}{kT}\right) \cdot \exp\left(\frac{q\Delta\phi_{BN}}{kT}\right) \cdot \exp(C_T E_M^2) \quad [2.19]$$

where C_T is a tunneling coefficient. A tunneling coefficient of $8 \times 10^{-13} \text{ cm}^2/\text{V}^2$ was found to yield an increase in leakage current by six orders of magnitude as shown in Fig. 2.9 consistent with the experimental observations. Thus, the inclusion of the tunneling model enhances the leakage current by another three orders of magnitude beyond that due to the Schottky barrier lowering phenomenon.

As discussed above, the leakage current in silicon carbide Schottky rectifiers increases much more rapidly with reverse voltage than in silicon devices. Fortunately, larger barrier heights can be utilized in silicon carbide devices when compared with silicon devices to reduce the absolute magnitude of the leakage current density because an on-state voltage drop of 1 to 1.5 volts is acceptable for such high voltage structures. This enables maintaining an acceptable level of power dissipation in the reverse blocking mode. For example, in the case of the 3kV 4H-SiC Schottky diode discussed above, the reverse power dissipation at room temperature is less than 1 W/cm^2 compared with an on-state power dissipation of 100 W/cm^2 . The expected increase in leakage current with temperature must of course be taken into account in order to ensure that the reverse power dissipation remains below the on-state power dissipation for stable operation. The leakage current can be suppressed by shielding the Schottky contact¹ using the JBS rectifier structure¹² originally proposed for silicon devices.

2.4 Summary

The physics of operation of the power Schottky rectifier structure has been described in this chapter to provide background information for the discussion of the advanced concepts in this book. For power devices with relatively high breakdown voltages, the dominant current conduction mechanism is by the thermionic emission process. For power Schottky rectifiers, it is necessary to include the impact of the series resistance of the drift region on the on-state voltage drop. This series resistance limits the performance of silicon rectifiers to a breakdown voltage of less than 100 volts. In addition, the Schottky barrier lowering and pre-breakdown avalanche multiplication must be taken into consideration when analyzing the leakage current for silicon devices because they can enhance the leakage current by an order of magnitude for high reverse bias voltages. In the case of silicon carbide

Schottky rectifiers, it is possible to extend the breakdown voltage to at least 3000 volts due to the much smaller resistance in the drift region. However, the reverse leakage current in silicon carbide devices is significantly enhanced by the tunneling current at high reverse bias voltages. The textbook³ should be consulted for a more detailed treatment of the basic power Schottky rectifier.

The leakage current in silicon and silicon carbide Schottky rectifiers can be suppressed by shielding the Schottky barrier to reduce the electric field at the metal-semiconductor interface. Various approaches to achieve this by using either P-N junctions, MOS-regions, or a second metal with larger barrier height are discussed in subsequent chapters of this book.

References

¹ B.J. Baliga, "Silicon Carbide Power Devices", World Scientific Publishing Company, Singapore, 2005.

² B.J. Baliga, "Power Semiconductor Devices for Variable Frequency Drives", Proceedings of the IEEE, Vol. 82, pp. 1112-1122, 1994.

³ B.J. Baliga, "Fundamentals of Power Semiconductor Devices", Springer Scientific, New York, 2008.

⁴ S.M. Sze, "Physics of Semiconductor Devices", pp. 254-258, 2nd Edition, John Wiley and Sons, 1981.

⁵ H.A. Bethe, "Theory of the Boundary Layer of Crystal Rectifiers", MIT Radiation Laboratory Report, Vol. 43, p. 12, 1942.

⁶ E.H. Rhoderick and R.H. Williams, "Metal-Semiconductor Contacts", Second Edition, pp. 35-38, Oxford Science Publications, 1988.

⁷ S.L. Tu and B.J. Baliga, "On the Reverse Blocking Characteristics of Schottky Power Diodes", IEEE Transactions on Electron Devices, Vol. 39, pp. 2813-2814, 1992.

⁸ M. Bhatnagar, P.K. McLarty, and B.J. Baliga, "Silicon Carbide High Voltage (400V) Schottky Barrier Diodes", IEEE Electron Device Letters, Vol. 13, pp. 501-503, 1992.

⁹ F. Dahlquist, et al, "A 2.8kV, Forward Drop JBS Diode with Low Leakage", Silicon Carbide and Related Materials – 1999, Material Science Forum, Vol. 338-342, pp. 1179-1182, 2000.

¹⁰ Y. Sugawara, K. Asano, and R. Saito, "3.6kV 4H-SiC JBS Diodes with Low Ron", Silicon Carbide and Related Materials – 1999, Material Science Forum, Vol. 338-342, pp. 1183-1186, 2000.

¹¹ T. Hatakeyama and T. Shinohe, "Reverse Characteristics of a 4H-SiC Schottky Barrier Diode", Silicon Carbide and Related Materials – 2001, Material Science Forum, Vol. 389-393, pp. 1169-1172, 2002.

¹² B.J. Baliga, "The Pinch-Rectifier: A Low Forward Drop, High Speed Power Diode", IEEE Electron Device Letters, Vol. EDL-5, pp. 194-196, 1984.



<http://www.springer.com/978-0-387-75588-5>

Advanced Power Rectifier Concepts

Baliga, B.J.

2009, XVI, 352 p. 310 illus., Hardcover

ISBN: 978-0-387-75588-5